Sweeting, S., Hall, C., Potticary, J., Pridmore, N. E., Warren, S. D., Cremeens, M. E., D'Ambruoso, G. D., Matsumoto, M., & Hall, S. R. (2020). The Solubility and Stability of Heterocyclic Chalcones Compared to Trans-chalcone. *Acta Crystallographica Section B*, *B76*(1), 13-17. https://doi.org/10.1107/S2052520619015907

research paper

Acta Cryst B STRUCTURAL SCIENCE CRYSTAL ENGINEERING MATERIALS

ISSN 2052-5206

The solubility and stability of heterocyclic chalcones compared with *trans*-chalcone

Stephen G. Sweeting,[a] Charlie L. Hall,[a] Jason Potticary,[a] Natalie E. Pridmore,[a] Stephen D. Warren,[b] Matthew E. Cremeens,[b] Gemma D. D'Ambruoso,[b] Masaomi Matsumoto[b] and Simon R. Hall[a]*

[a]School of Chemistry, University of Bristol, Cantock's Close, Bristol, Somerset BS8 1TS, UK, and [b]Department of Chemistry and Biochemistry, Gonzaga University, Boone Avenue, Spokane, Washington 99258, USA. *Correspondence e-mail: simon.hall@bristol.ac.uk

Received 15 October 2019
Accepted 25 November 2019

Edited by A. J. Blake, University of Nottingham, England

Keywords: crystal structure; heterocyclic chalcones; solubility; thermal stability; intermolecular interactions; chalcones; crystals.

CCDC reference: 1952662

Supporting information: this article has supporting information at journals.iucr.org/b

Heterocyclic chalcones are a recently explored subgroup of chalcones that have sparked interest due to their significant antibacterial and antifungal capabilities. Herein, the structure and solubility of two such compounds, (*E*)-1-(1*H*-pyrrol-2-yl)-3-(thiophen-2-yl)prop-2-en-1-one and (*E*)-3-phenyl-1-(1*H*-pyrrol-2-yl)prop-2-en-1-one, are assessed. Single crystals of (*E*)-1-(1*H*-pyrrol-2-yl)-3-(thiophen-2-yl)prop-2-en-1-one were grown, allowing structural comparisons between the heterocyclic chalcones and (2*E*)-1,3-diphenylprop-2-en-1-one, trivially known as *trans*-chalcone. The two heterocyclic chalcones were found to be less soluble in all solvents tested and to have higher melting points than *trans*-chalcone, probably due to their stronger intermolecular interactions arising from the functionalized rings. Interestingly, however, it was found that the addition of the thiophene ring in (*E*)-1-(1*H*-pyrrol-2-yl)-3-(thiophen-2-yl)prop-2-en-1-one increased both the melting point and solubility of the sample compared with (*E*)-3-phenyl-1-(1*H*-pyrrol-2-yl)prop-2-en-1-one. This observation may be key for the future crystal engineering of heterocyclic chalcones for pharmaceutical applications.

1. Introduction

1,3-Diarylprop-2-en-1-ones, trivially known as chalcones, are organic molecules which feature two aromatic rings linked by an enone backbone. The name 'chalcone' is derived from the Greek word *chalkos*, which translates as 'copper', since the majority of naturally occurring chalcones have this colour (Sahu *et al.*, 2012). Chalcones have a variety of uses, ranging from being pharmacophores (Onyilagha *et al.*, 1997), acting as nematicides (Simmonds *et al.*, 1990), and in the synthesis of other more complex compounds (Lasri & Ismail, 2018; Zhuang *et al.*, 2017). For example, chalcones are used as reactants in the Robinson annulation for ringed compounds (Safaei-Ghomi & Alishahi, 2006). In addition to their pharmaceutical applications, some chalcones are known to be fluorescent when the aromatic rings are functionalized with electron-donating groups, affording them the potential to be used as probes for mechanistic investigations (Zhuang *et al.*, 2017). Chalcones can be synthesized in a variety of ways, including Friedel–Crafts acylations (Shotter *et al.*, 1978), palladium cross-coupling reactions (Eddarir *et al.*, 2003) and using the Wittig reaction between an appropriate aromatic aldehyde and ylide (Xu *et al.*, 1995).

Chalcones which contain a pyrrole, thiophene or furan aromatic ring instead of the traditional phenyl ring are known as heterocyclic chalcones and are of interest because of their enhanced pharmacophoric properties. For example, when

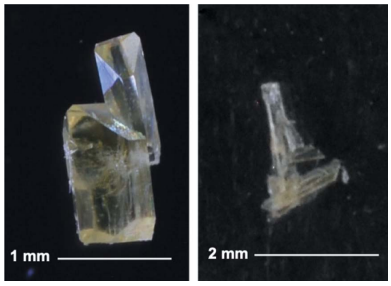

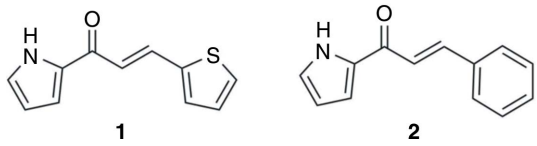

1 **2**

Figure 1
Skeletal formulae for the two heterocyclic chalcones studied here. **1** is (*E*)-1-(1*H*-pyrrol-2-yl)-3-(thiophen-2-yl)prop-2-en-1-one and **2** is (*E*)-3-phenyl-1-(1*H*-pyrrol-2-yl)prop-2-en-1-one.

combined with antibiotics like benzylpenicillin (penicillin G), heterocyclic chalcones featuring the furan functional group instead of the traditional phenyl ring show significantly greater antibacterial activity against *Bacillus subtilis*, *Escherichia coli* and *Staphylococcus aureus* (Sridhar *et al.*, 2011; Tran *et al.*, 2012). Little has been reported on the uses of unsubstituted heterocyclic chalcones, however. From this perspective, fully characterizing the intermolecular interactions involved in these compounds is vital as they relate to emergent properties such as solubility, which are critical in engineering materials with desired properties for pharmaceutical applications.

In this article, the solubility limits of two heterocyclic chalcones (Fig. 1) and *trans*-chalcone are deduced for a variety of polar and non-polar solvents. The crystal structure of **1** was solved via single-crystal X-ray diffraction for the first time and is compared with that of **2** (Gong *et al.*, 2008) and *trans*-chalcone (Wu *et al.*, 2006). Analysis of these molecules in the solid state highlights the stark differences in their intermolecular interactions, providing an insight into their solubilities. Compound **2** and the polymorphs of *trans*-chalcone were verified using X-ray powder diffraction and matched with the previously reported structures. The thermal properties of the two heterocyclic chalcones were collected and compared with that of *trans*-chalcone in order to demonstrate the differences in intermolecular interaction strength.

2. Synthesis of heterocyclic chalcones and crystal growth

Heterocyclic chalcones **1** and **2** were synthesized using the Claisen–Schmidt condensation (see the supporting information for detailed experimental information; ^{1}H and ^{13}C NMR spectra for both **1** and **2** are shown in Figs. S1–S6). Single crystals of **1** and **2** were grown from *n*-hexane, toluene, tetrahydrofuran (THF), ethyl acetate, chloroform, acetone, ethanol and methanol at a concentration of 0.05 mol dm^{-3} by slow evaporation (Figs. S7 and S8 in the supporting information). This was achieved by covering the solutions with Parafilm and piercing the film with a small hole, approximately 2 mm in diameter. The solutions were left at room temperature (295 K) for two weeks to allow all the solvent to evaporate. After growth from slow evaporation, larger crystals of both heterocyclic chalcones exhibited a pale-yellow colour similar to that of *trans*-chalcone, although thinner crystals appeared colourless. Crystals of **1** tended to adopt a block-like morphology (Fig. 2), whereas **2** tended to form both needle and plate-like structures. The single crystal of **1** grown from THF was used for single-crystal X-ray diffraction.

Table 1
Solubility limits of all three chalcones at 295 K in order of solvent polarity to three significant figures.

Units for the solubility limits are mg ml^{-1}. Errors are to two significant figures. Refer to Table S1 in the supporting information for further information.

Solvent (polarity index)†	*trans*-Chalcone	**1**	**2**
n-Hexane (0.009)	44.0 ± 1.0	Insoluble	Insoluble
Toluene (0.099)	630 ± 5.1	Insoluble	14.0 ± 0.74
THF (0.207)	1010 ± 8.1	213 ± 1.7	105 ± 0.91
Ethyl acetate (0.228)	855 ± 6.9	49.5 ± 0.53	50.0 ± 2.1
Chloroform (0.259)	730 ± 5.9	65.5 ± 0.63	51.0 ± 1.1
Acetone (0.355)	1050 ± 8.4	101 ± 0.88	82.0 ± 3.0
Ethanol (0.654)	175 ± 1.4	9.00 ± 0.36	11.0 ± 0.73
Methanol (0.762)	130 ± 1.1	15.5 ± 0.37	10.5 ± 0.36

† The values for relative polarity are normalized from measurements of solvent shifts of absorption (Reichardt & Welton, 2011).

3. Solubility of the heterocyclic chalcones compared with *trans*-chalone

The solubility limits of the chalcones being considered here were found by forming saturated solutions using the solvents listed in Table 1, using a method which has been described previously (experimental details can be found in the supporting information; Salman *et al.*, 2015). Powder X-ray diffraction was used initially, to assure that the crystal structures of the samples being tested were consistent. The solubilities of the three chalcones in Table 1 show that all three dissolved well in polar solvents such as THF and acetone, relative to non-polar solvents such as *n*-hexane and toluene.

Solubility relies on three sets of intermolecular interactions: solute–solute, solvent–solvent and solute–solvent. If the enthalpy associated with the formation of solute–solvent interactions is greater than the sum of the enthalpies for solute–solute and solvent–solvent interactions, then the solute will dissolve into the solvent. Overall, the heterocyclic chalcones are much less soluble than *trans*-chalcone in all the solvents tested. This will predominantly be caused by the weaker solute–solute interactions between the *trans*-chalcone molecules compared with the interactions between the

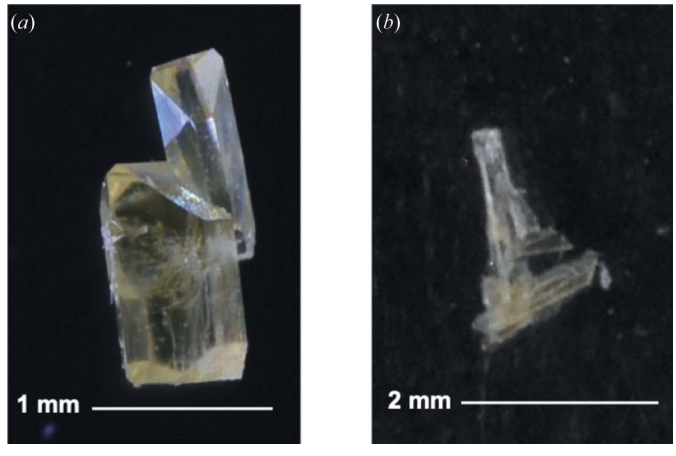

Figure 2
Crystals of (*a*) **1** and (*b*) **2**, grown using the slow evaporation method from methanol at a concentration of 0.05 mol dm^{-3}.

heterocyclic chalcone molecules. In order to confirm this, the polarities of the three chalcones were calculated. Molecules of each chalcone were optimized using density functional theory (DFT) in *GAUSSIAN09* (Frisch *et al.*, 2009) with the B3LYP functional set to the 6-31G level (Xue & Gong, 2009). For **1**, there are two different conformers which depend on the location of the sulfur atom, being either *syn* or *anti* with respect to the carbonyl group. This is reflected by the disorder within the crystal structure and so a weighted average was used to calculate the polarity of **1**, based on the polarity of both conformers. *trans*-Chalcone was calculated to be the most polar of the three chalcones being considered (3.36 D), followed by **2** (1.98 D) and then **1** as the least polar (1.56 D). The decrease in polarity associated with the heterocyclic chalcones results in a decrease in solubility for the non-polar solvents *n*-hexane and toluene, as shown in Table 1.

The functionalized rings found in **1** and **2** provide a greater variety of intermolecular interactions between each other, which increases the solute–solute interactions and in turn reduces their solubility compared with *trans*-chalcone. When comparing **1** and **2**, the solubility of **1** is greater in polar aprotic solvents than that of **2**. This is probably due to the lone pair featured on the thiophene ring of **1** providing more intermolecular interactions with the aprotic solvent than **2** is able to do.

Chalcone **2** is generally less soluble than **1** in all tested solvents, except toluene and ethanol. The differences in solubility can be elucidated by looking at the molecular electrostatic potentials of the three chalcones (Fig. 3 and Fig. S9 in the supporting information). The solubility of *trans*-chalcone and **2** in toluene is probably due to a favourable interaction involving the non-heterocyclic phenyl ring, which is not present in **1**. Solubility in protic solvents such as ethanol and methanol should be similar for both heterocyclic chalcones, as the solute–solvent interactions will be mediated predominantly via the carbonyl group.

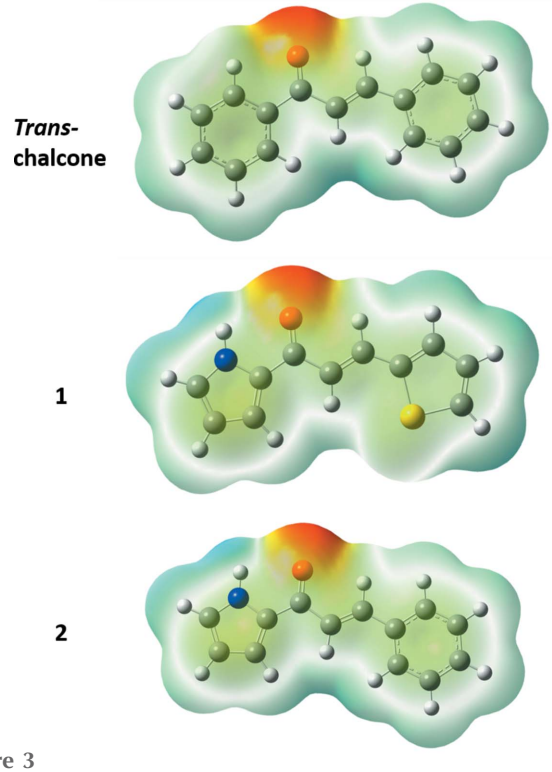

Figure 3
Molecular electrostatic potentials for *trans*-chalcone, **1** and **2**. The range for all three plots is between -6.5×10^{-2} a.u. (red) to 6.5×10^{-2} a.u. (blue), with an isovalue of MO = 0.02 e Å^{-3} and a density of 0.0004.

4. Stability of the heterocyclic chalcones compared with *trans*-chalcone

Thermal analysis using differential scanning calorimetry (DSC) indicates that the melting points of **1** and **2** are 423.42 and 410.95 K, respectively (Figs. S10–S12). On recrystallization from the melt, a different polymorph of *trans*-chalcone formed, resulting in two separate melting points being recorded (Fig. 4). The first melting occurred at 330.24 K (form I, verified with powder X-ray diffraction in Figs. S13–S16) and the second at 325.95 K (form II, verified with powder X-ray diffraction in Figs. S17–S20).

The use of heterocyclic rings in both **1** and **2** increases the stability of the chalcone, indicated by **1** and **2** having significantly higher melting points than *trans*-chalcone, implying stronger intermolecular interactions between the chalcone molecules of **1** and **2**. The crystal structures of both **1** and **2** have similar hydrogen-bonding motifs (Fig. 5; see also Figs. S21–S29, and Tables S2 and S3 for single-crystal and powder XRD data relating to **1** and powder XRD data relating to **2**). The distance between the donor pyrrole and the acceptor carbonyl functional groups in the crystal structures of both **1** and **2** are 2.832 Å or 2.841 Å, and 2.817 Å, respectively, which are approximately the length of a short hydrogen-bond interaction found in the secondary structure of proteins

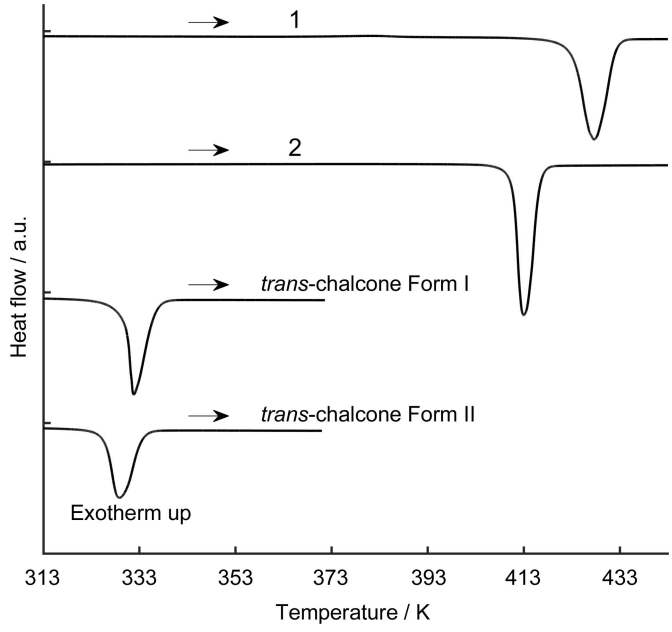

Figure 4
The DSC heating cycles for all three chalcones being considered, in the temperature range 313 to 453 K.

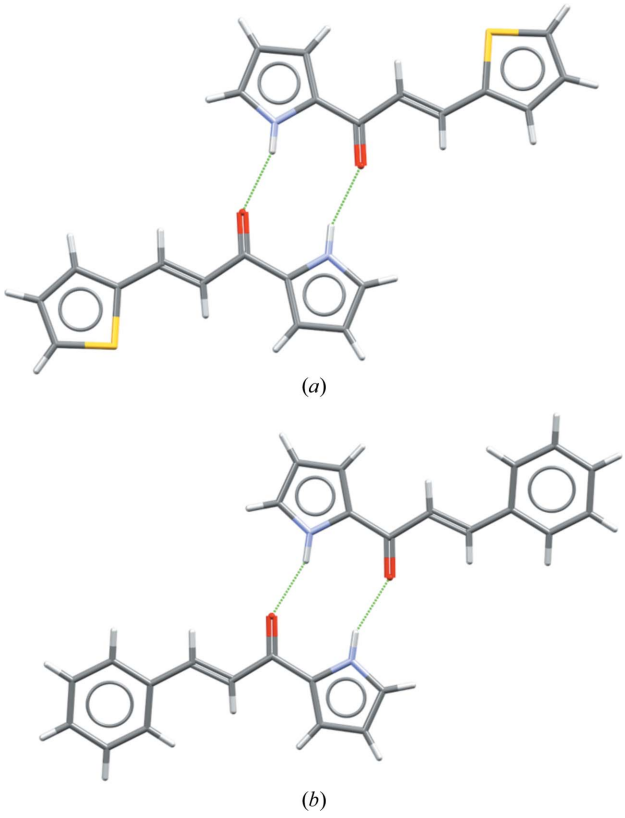

Figure 5
Two molecules each of (*a*) **1** and (*b*) **2**, showing the hydrogen bonding (green lines) within their crystal structures. The visualization software that was used was *Mercury 4.1.3* (Macrae *et al.* 2006, 2008).

(Langkilde *et al.*, 2008). Form I of *trans*-chalcone features no hydrogen bonding within its crystal structure; but form II does, between the carbonyl group and the phenyl ring in the third position on the enone backbone (Wu *et al.*, 2006). The hydrogen-bonding interactions in **1** and **2** are stronger than those found in *trans*-chalcone form II due to the nitrogen atom having a higher electronegativity than carbon. This will result in a higher melting point for the heterocyclic chalcones, which we have observed here via DSC.

Though the hydrogen bonding for **1** and **2** is similar, the melting point is higher for **1** than for **2**, suggesting there is another significant intermolecular interaction to consider. Both **1** and **2** feature L-shaped arrangements in the molecular packing (Fig. 6), suggesting that π interactions also play a role in stabilizing the structure. In **1**, the thiophene and pyrrole rings appear to adopt an L-shaped arrangement with similar rings on adjacent molecules, which relies on a lone-pair–π interaction for the thiophene rings [the interaction covers a distance of 3.636 (5) Å] and an H–π interaction for the pyrrole rings [the interaction covers a distance of 2.877 (2) Å]. In **2**, the phenyl and pyrrole rings form an L-shaped arrangement between each other in adjacent molecules, which arise from H–π interactions (the interactions cover 3.122 (2) Å for benzene–benzene interactions and 5.327 (3) Å for benzene–pyrrole interactions). However, the interaction distances are greater in **2** than **1** and the π interactions in **2** do not lie within the van der Waals radii of the atoms, where hydrogen is recorded to have a van der Waals radius of 1.68 Å, carbon 1.30 Å and sulfur 1.83 Å (Mantina *et al.*, 2009).

To estimate the strengths of the L-shaped arrangements in both heterocyclic chalcone crystal structures, the dissociation energies of the t-shaped dimer equivalent between the benzene, pyrrole and thiophene rings were compared using values which are recorded in the literature. Comparing the dissociation energies of the benzene–benzene and thiophene–thiophene t-shaped dimers, the thiophene–thiophene dimer has a larger dissociation energy than the benzene analogue, reported to be −2.60 and −2.46 kcal mol^{-1} (1 kcal mol^{-1} = 4.184 kJ mol^{-1}), respectively (Tsuzuki *et al.*, 2002). This is due to the high polarizability of the sulfur atom in the thiophene ring, increasing the dispersion forces between the two heterocyclic rings which in turn increases the strength of the dimer interaction (Tsuzuki *et al.*, 2002). As the hydrogen-bonding interactions are very similar for both **1** and **2**, it seems most likely that the differences in stability are primarily due to the differences in the energy of the t-shaped arrangements of the aromatic rings and therefore the interactions with the π systems of the aromatic rings.

Form II of *trans*-chalcone is also reported to feature t-shaped H–π interactions within its crystal structure between the phenyl rings (Wu *et al.*, 2006). Even though the t-shaped dimer for the benzene–benzene system is stronger than that for the benzene–pyrrole system found in **2**, due to the nitrogen atom being less polarizable than carbon, *trans*-chalcone form II is much less stable than **2** due to the hydrogen-bonding interactions being weaker. Form I of *trans*-chalcone features arrangements which are similar to a stacked π–π interaction between the phenyl rings. Though the displaced stacked dimer

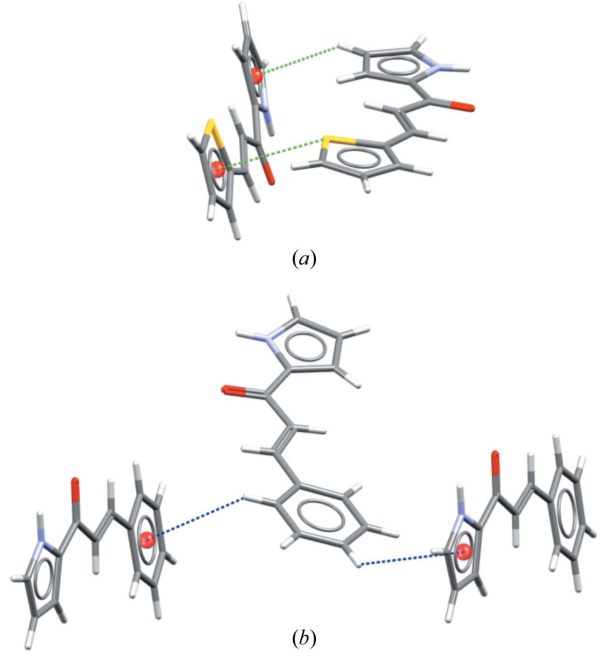

Figure 6
Molecules of (*a*) **1** and (*b*) **2**, showing key π interactions. Orange spheres represent the centroids of the aromatic rings. Compound **1** shows lone-pair–π interactions between the thiophene rings and H–π interactions between pyrrole rings. Compound **2** shows H–π interactions.

for benzene has a slightly larger dissociation energy than the t-shaped dimer [reported to be -2.48 kcal mol^{-1}; (Tsuzuki *et al.*, 2002)], the dissociation energy is still smaller than that for the t-shaped thiophene dimer which has a dissociation energy of -2.60 kcal mol^{-1} (Tsuzuki *et al.*, 2002). This reduces the stability of the polymorph when compared with the heterocyclic chalcones.

5. Conclusion

In conclusion, the heterocyclic chalcones investigated here are less soluble than *trans*-chalcone due to the weak solute–solute interactions present in *trans*-chalcone's molecular packing, highlighted by large differences in melting points when compared with **1** and **2**.

Within the heterocyclic chalcone crystal structures, there are two main bonding motifs, hydrogen bonding and t-stacked dimer arrangements, which involve interactions with the π system of the heterocyclic rings. In both **1** and **2**, the hydrogen bonding is similar, but the thiophene group leads to a more stable t-shaped arrangement in **1**, which correlates with a higher melting temperature. Interestingly, however, **1** is still more soluble than **2** in the majority of polar solvents tested here, which suggests that the increase in solute–solute interactions does not overcome the additional solute–solvent interactions arising from the extra heterocyclic ring.

The results found may apply to the design and synthesis of more pharmaceutically attractive heterocyclic chalcones, tuning both the stability of the compound and its solubility simultaneously. The heterocyclic chalcones may also be suitable for interactions with proteins if they are found to feature bioactivity.

6. Related literature

For further literature related to the supporting information, see Bruker (2001, 2007), Dolomanov *et al.* (2009), Frisch *et al.* (2009), Macrae *et al.* (2006), Palatinus & Chapuis (2007), Palatinus *et al.* (2012), Reichardt & Welton (2011) and Sheldrick (2008, 2015).

Acknowledgements

The authors would like to thank the following people at Gonzaga University: Elisabeth Mermann-Jozwiak, Jeff Hazen, Scott Economu, Julia Talarico, Brett Hendricks, and the summer 2019 CHEM 230L students for their assistance. We gratefully acknowledge financial support provided by a grant from the Howard Hughes Medical Institute through its Undergraduate Science Education Program for the acquisition of some of our equipment.

Funding information

SRH, JP and CLH acknowledge the Engineering and Physical Sciences Research Council UK (grant EP/L015544/1), MagnaPharm, a collaborative research project funded by the European Union's Horizon 2020 Research and Innovation programme (H2020 Future and Emerging Technologies; grant No. 736899), and the Centre for Doctoral Training in Condensed Matter Physics for project funding.

References

Bruker (2001). *SADABS*. Bruker AXS Inc., Madison, Wisconsin, USA.
Bruker (2007). *SAINT+ Integration Engine*. Bruker AXS Inc., Madison, Wisconsin, USA.
Dolomanov, O. V., Bourhis, L. J., Gildea, R. J., Howard, J. A. K. & Puschmann, H. (2009). *J. Appl. Cryst.* **42**, 339–341.
Eddarir, S., Cotelle, N., Bakkour, Y. & Rolando, C. (2003). *Tetrahedron Lett.* **44**, 5359–5363.
Frisch, M. J. *et al.* (2009). *GAUSSIAN09*. Gaussian Inc., Wallingford, Connecticut, USA.
Gong, Z.-Q., Liu, G.-S. & Xia, H.-Y. (2008). *Acta Cryst.* E**64**, o151.
Langkilde, A., Kristensen, S. M., Lo Leggio, L., Mølgaard, A., Jensen, J. H., Houk, A. R., Navarro Poulsen, J.-C., Kauppinen, S. & Larsen, S. (2008). *Acta Cryst.* D**64**, 851–863.
Lasri, J. & Ismail, A. I. (2018). *Indian J. Chem. B.* **57**, 362–373.
Macrae, C. F., Bruno, I. J., Chisholm, J. A., Edgington, P. R., McCabe, P., Pidcock, E., Rodriguez-Monge, L., Taylor, R., van de Streek, J. & Wood, P. A. (2008). *J. Appl. Cryst.* **41**, 466–470.
Macrae, C. F., Edgington, P. R., McCabe, P., Pidcock, E., Shields, G. P., Taylor, R., Towler, M. & van de Streek, J. (2006). *J. Appl. Cryst.* **39**, 453–457.
Mantina, M., Chamberlin, A. C., Valero, R., Cramer, C. J. & Truhlar, D. G. (2009). *J. Phys. Chem. A*, **113**, 5806–5812.
Onyilagha, J. C., Malhotra, B., Elder, M., French, C. J. & Towers, G. H. N. (1997). *Can. J. Plant Pathol.* **19**, 133–137.
Palatinus, L. & Chapuis, G. (2007). *J. Appl. Cryst.* **40**, 786–790.
Palatinus, L., Prathapa, S. J. & van Smaalen, S. (2012). *J. Appl. Cryst.* **45**, 575–580.
Reichardt, C. & Welton, T. (2011). *Solvents and Solvent Effects in Organic Chemistry*, 4th ed. Weinheim: Wiley–VCH.
Safaei-Ghomi, J. & Alishahi, Z. (2006). *Org. Prep. Proced. Int.* **38**, 417–422.
Sahu, N. K., Balbhadra, S. S., Choudhary, J. & Kohli, D. V. (2012). *Curr. Med. Chem.* **19**, 209–225.
Salman, M. A., Al-Nuwaibit, G., Safar, M. & Al-Mesri, A. (2015). *Int. J. Emerg. Technol. Adv. Eng.* **5**, 1–7.
Sheldrick, G. M. (2008). *Acta Cryst.* A**64**, 112–122.
Sheldrick, G. M. (2015). *Acta Cryst.* C**71**, 3–8.
Shotter, R. G., Johnston, K. M. & Jones, J. F. (1978). *Tetrahedron*, **34**, 741–746.
Simmonds, M. S. J., Blaney, W. M., Delle Monache, F. & Marini Bettolo, G. B. (1990). *J. Chem. Ecol.* **16**, 365–380.
Sridhar, S., Dinda, S. C. & Prasad, Y. R. (2011). *E-J. Chem.* **8**, 541–546.
Tran, T. D., Nguyen, T. T., Do, T. H., Huynh, T. N., Tran, C. D. & Thai, K. M. (2012). *Molecules*, **17**, 6684–6696.
Tsuzuki, S., Honda, K. & Azumi, R. (2002). *J. Am. Chem. Soc.* **124**, 12200–12209.
Wu, M. H., Yang, X. H., Zou, W. D., Liu, W. J. & Li, C. (2006). *Z. Kristallogr. New Cryst. Struct.* **221**, 323–324.
Xu, C. D., Chen, G. Y. & Huang, X. (1995). *Org. Prep. Proced. Int.* **27**, 559–561.
Xue, Y. S. & Gong, X. D. (2009). *J. Mol. Struct. Theochem*, **901**, 226–231.
Zhuang, C. L., Zhang, W., Sheng, C. Q., Zhang, W. N., Xing, C. G. & Miao, Z. Y. (2017). *Chem. Rev.* **117**, 7762–7810.